

New heights for hard disk drives

by Jian-Gang (Jimmy) Zhu

To this day, hard disk drives (HDDs) remain the only archival mass data storage device in a computer. The first disk drive, called RAMAC (random access method of accounting and control), was developed for the IBM 350 computer in 1957¹. Over the past decade, as the demands for digital data have exploded, the storage capacity of HDDs has grown at a matching rate, if not faster. Today, a 3.5" HDD has a capacity of 160 GB, capable of storing nearly a thousand times more data than a HDD of the same size just ten years ago. The area storage density of a disk surface in a RAMAC was only 2 kbit/in². It is now 60 Gbit/in², a 30 million-fold increase over the past 46 years with an average annual growth rate of nearly 80% during the last ten years. Recent demonstrations have shown area recording densities² as high as 150 Gbit/in².

Such tremendous storage density growth has permitted the HDD to be made much smaller. The very first generation of HDDs had dimensions on the scale of a storage cabinet, whereas the micro-drive developed by IBM in 2000 was small enough to fit in an eggshell and had a storage capacity over 1 GB.

The technologies involved in building a HDD are truly interdisciplinary, including coding and signal processing, electromagnetics, materials science and engineering, magnetism, microfabrication, electronics, tribology, control systems, heat transfer, and so on. However, the scope of this article will be limited to the magnetic aspect of data storage and retrieval mechanisms in a HDD.

Storing bits

In a HDD, binary data are stored in a thin magnetic layer, called the recording medium, deposited on a substrate. A '1' bit is stored as a local magnetic moment reverses its orientation along the circumferentially arranged data track – the magnetization transition, whereas a '0' bit corresponds to no change of the local moment orientation (Fig. 1). Since the magnetic moment orientation representing the stored bits is in the direction of the recording track, this mode is referred to as longitudinal recording (Fig. 2). Magnetic hysteresis of the recording media enables the retention of the local magnetic moment orientation and, thereby, data. The disk rotates at a constant speed, which ranges from 3600 rpm in a low-end product to 15 000 rpm in a high-end product. Meanwhile a recording head, consisting of both write and read elements embedded at the end of an air-bearing slider, flies over the disk surface at a steady clearance of 5 nm. The

Department of Electrical and Computer Engineering
and Data Storage Systems Center,
Carnegie Mellon University,
Pittsburgh, PA 15213-3890
Tel: +1 412 268 8373
Fax: +1 412 268 8554
E-mail: jzhu@ece.cmu.edu

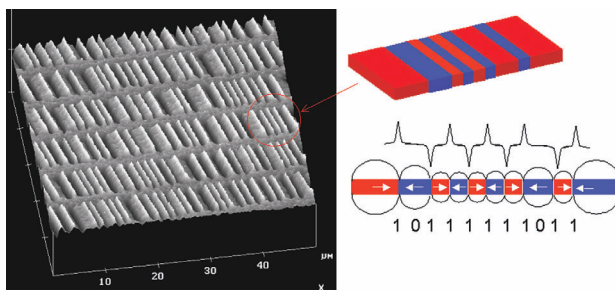


Fig. 1 A magnetic force micrograph of a disk media recorded in a commercial HDD. The peaks and valleys represent the magnetic flux generated from north- and south-pole transitions, respectively. A transition in the medium represents a '1' bit, while a missing transition represents a '0' bit.

write element, an inductive magnetic transducer, produces a field that magnetizes the medium in the vicinity of the head gap. During writing, the current amplitude is kept constant, while the direction is reversed every time a bit is stored.

The reversal of the current direction in a write head yields a corresponding reversal in the head field direction. This results in a reversal of the magnetization orientation in the medium over the region where the field is greater than the coercivity of the medium. This region is referred to as the recording zone or bubble (Fig. 3). Every time the write current reverses direction, a bit is stored as a magnetic transition. The transition is never infinitely sharp and always has a finite length because of the head field gradient, the slope of the medium hysteresis loop at coercivity, and the demagnetizing field arising from the magnetic poles generated in the transition. The transition length parameter a , equal to half the length of the transition zone, as shown in Fig. 3, can be calculated according to the following equation^{3,4},

$$a = \frac{(1 - S^*)(d + T/2)}{\pi Q} + \sqrt{\left(\frac{(1 - S^*)(d + T/2)}{\pi Q}\right)^2 + \frac{4M_r T(d + T/2)}{Q H_c}}$$

where Q is a constant related to head geometry. Thus, to increase the linear density, i.e. the number of bits per unit distance along the data track, the transition length parameter has to be reduced. History has shown that any increase of the area recording density is always accompanied by a reduction in the head-medium separation d , the medium thickness T , and the medium moment M_r , in addition to an increase of the medium coercivity H_c .

Raising write head fields

To achieve the optimum transition sharpness, the field magnitude needs to be optimized such that its gradient at the center of the transition is a maximum. This means that

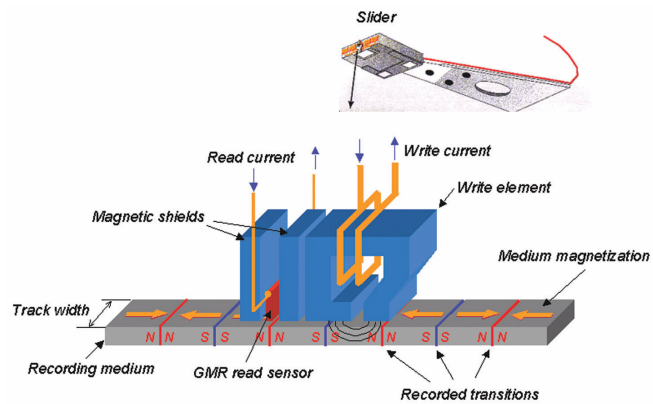


Fig. 2 Longitudinal recording scheme used in current HDDs. The recording head consists of an inductive write element and a giant magnetoresistive read element. The stray field generated at the write element gap magnetizes the medium along the recording track.

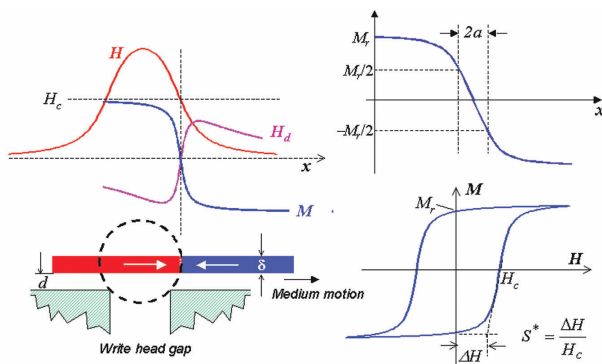


Fig. 3 Schematic of the writing of a transition. The recording geometry is shown bottom left. Within the dashed circle, referred to as the recording bubble, the head field magnitude along the recording direction is greater than the medium coercivity, H_c . A transition is created at the trailing edge of the bubble. H_d is the demagnetization field arising from the magnetic poles in the transition. The hysteresis loop of the recording medium is shown bottom right.

the maximum write head field in the medium has to be approximately twice the coercivity. The field generated by a write head is determined by the magnetic flux density inside the head poles at the gap. In current HDDs, the maximum head field is slightly less than half the magnetic flux density in the head poles. Over the years, the head pole material in the gap region has changed from permalloy ($Ni_{81}Fe_{19}$) with saturation flux density $B_s = 1.0$ T, to $Ni_{45}Fe_{55}$ with $B_s = 1.5$ T, to $Fe_{65}Co_{35}$ alloy with $B_s = 2.45$ T, which is used in write heads manufactured today⁵⁻⁷. At the same time, the coercivity of thin film recording media has increased from 2000 Oe to 4800 Oe. However, the alloy $Fe_{65}Co_{35}$ used in today's write heads has the highest saturation magnetic flux density ($B_s = 2.45$ T) of any existing magnetic material. This means that the maximum write field inside recording media in longitudinal mode is limited to 1.2 T. As an estimate, data

writing in a medium where coercivity exceeds 6000 Oe would not be optimal.

As shown in Fig. 2, the field in the recording medium is the fringing field generated across the head gap by the magnetized write head poles on both sides. Inside the gap, the magnetic flux density is essentially the same as that inside the magnetic poles on both sides of the gap, almost twice the fringing flux density. However, if the gap material is superconducting (this is a big 'if'), the magnetic flux is repelled out of the gap and the field intensity in the recording media would be more than doubled.

To achieve sufficient writing efficiency, which is defined as

$$\varepsilon = \frac{\text{field intensity in gap} \times \text{gap length}}{\text{number of turns} \times \text{current amplitude}}$$

the head material needs to be reasonably soft, i.e. its permeability must be sufficiently high and its coercivity sufficiently small so that the field intensity within the head pole and yoke becomes negligible. It has been found that depositing a crystalline, body-centered cubic (bcc) Fe₆₅Co₃₅ film on top of a face-centered cubic (fcc) underlayer, such as Cu, yields very small grains with low coercivity⁸.

Spin valve read sensors

As shown in Fig. 4, the increase in area recording density over the past decade can be partially attributed to the reduction in magnetic moment density in the recording media. What made such a reduction possible was the utilization of magnetoresistive (MR) and, later, giant magnetoresistive

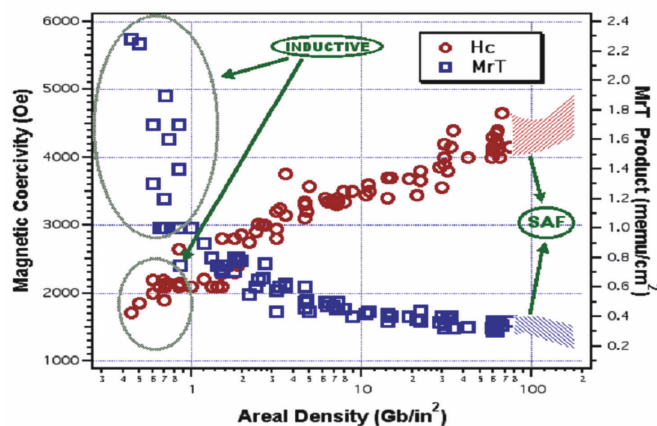


Fig. 4 Coercivity and moment density of thin film recording media in HDDs over the past 15 years versus corresponding area recording density. The area density increase has been facilitated by increased coercivity and decreased remanent magnetic moment density. (Courtesy of Gerardo Bertero and Komag Inc.)

(GMR) read sensors in HDDs, which have a superior magnetic sensitivity compared with the inductive read heads used prior to 1991. For both MR and GMR heads, magnetic flux arising from the recorded transitions in the medium produces a magnetization rotation of the sensing magnetic layer, the 'free layer', resulting in a resistance change in the sensing element. Here, only GMR heads, in particular spin valve heads, which replaced MR heads in HDD products eight years ago, will be discussed.

In 1988, the GMR effect was discovered in a {Fe/Cr}_n magnetic multilayer film epitaxially grown on a GaAs single crystal substrate⁹. It was found that a change of relative magnetic moment orientation between adjacent magnetic layers results in a significant change in resistance. When the layers are magnetized in parallel, the resistance is at a minimum. When the magnetizations of the adjacent magnetic layers are antiparallel to each other, the resistance is at a maximum. A resistance change of nearly 25% at room temperature and 100% at 4.2 K was recorded. In less than ten years, the first commercial HDDs with spin valve sensors^{10,11} utilizing the GMR effect rolled off the production line. The short time from discovery to commercial application is truly amazing compared with the 90 years it took for a practical use of the MR effect to be realized.

A simple spin valve read sensor (Fig. 5) consists of a GMR trilayer (two ferromagnetic layers separated by a nonmagnetic metallic interlayer), adjacent to an antiferromagnetic layer¹⁰⁻¹². A common example is NiFe/Cu/CoFe/PdPtMn (PdPtMn is the antiferromagnetic

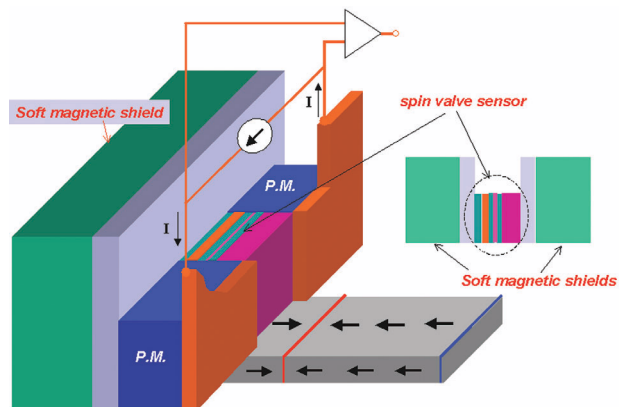


Fig. 5 Schematic of a spin valve head structure used in HDDs. A spin valve read sensor stack is placed in between a pair of permanent magnets that provide a horizontal magnetic field in the cross-track direction. Two soft magnetic shields are placed in the down track direction, enabling adequate spatial resolution for high linear recording density.

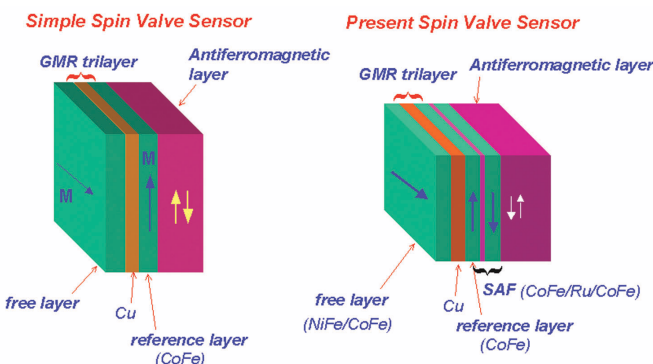


Fig. 6 Schematic of a simple spin valve read sensor stack and a spin valve with a synthetic antiferromagnet (SAF). The magnetic flux closure within the SAF is clearly advantageous for eliminating stray field in the free layer.

layer). The ferromagnetic layer adjacent to the antiferromagnetic layer is called the pinned layer because its magnetic moment is 'pinned' by a unidirectional magnetic field arising from the antiferromagnetic layer interface. This unidirectional field is often referred to as the exchange bias field¹³. For a spin valve read sensor in a HDD, the pinning direction is perpendicular to the air-bearing surface. The other ferromagnetic layer in the spin valve, the free layer, has its magnetic moment 'free' to sense the magnetic field flux from recorded transitions in the medium (Fig. 6). Driven by the magnetic field from a transition, the magnetic moment of the free layer rotates while the magnetic moment of the pinned layer maintains its direction as a reference. The resistivity of the sensor stack changes as the magnetization angle, θ , between the free and pinned layers changes,

$$\rho = \rho_0 + \Delta\rho \cdot \frac{1}{2} \cos\theta = \rho_0 \left(1 + \frac{\Delta\rho}{\rho_0} \cdot \frac{1}{2} \cos\theta \right)$$

where $\Delta\rho/\rho_0$ is the GMR ratio, which is ~6-8% for a simple NiFe/Cu/CoFe/PtMn structure, a figure of merit for sensor signal-to-noise ratio¹⁴. Ideally, the magnetization of the free layer should always be uniform so that when sensing recorded transitions magnetization rotation in the free layer is coherent. While sensing transitions (Fig. 6), the spin valve sensor produces a resistivity change (either an increase or decrease). With a current source connected to the sensor (Fig. 5), the passage of a transition under the spin valve sensor yields a voltage pulse with the polarity determined by the sign of the magnetic poles of the transition. To ensure that positive and negative voltage pulses have the same amplitude, the magnetization of the free layer at the

quiescent state is designed to be horizontal, orthogonal to the magnetization of the pinned layer.

The underlying physical mechanism of the GMR effect is the spin dependent electric transport in ferromagnetic transition metals (Fig. 7). For transition elements such as Fe, Co, and Ni, each atom has two conduction ($4s^2$) electrons, one with its spin magnetic moment parallel to the spontaneous magnetization of the material (a spin-up electron) and the other antiparallel (a spin-down electron). The resistance of the material arises from diffusive scattering of the electrons. In Fe, Co, or Ni, the scattering rate of a spin-up electron is different to that of a spin-down electron. One can consider the current carried by spin-up and spin-down electrons separately – a model referred to as the two-current model¹⁵. The normalized difference between the resistivity of the spin-up and spin-down channels,

$$P = \frac{\rho_{\downarrow} - \rho_{\uparrow}}{\rho_{\downarrow} + \rho_{\uparrow}}$$

is defined as the polarization factor. Spin valve sensors made from materials with a higher polarization factor can potentially have a higher GMR ratio. For example¹⁶, the permalloy Ni₈₁Fe₁₉ has a polarization factor of 0.25, while

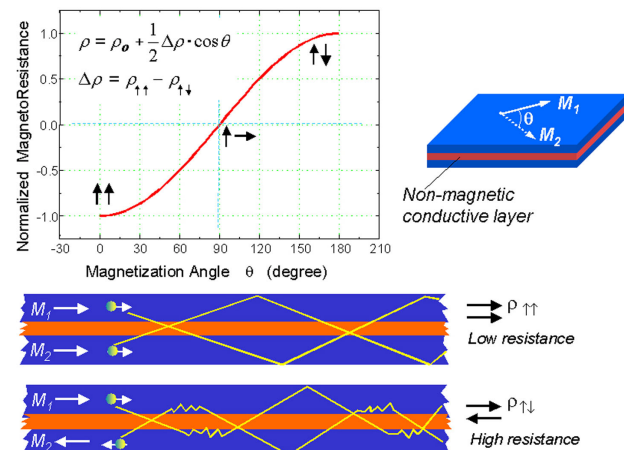


Fig. 7 GMR effect in Co/Cu/Co. The resistance of the trilayer is a function of the relative magnetization orientation between the two layers. The GMR effect arises from the spin dependent electric transport in the ferromagnetic material. In Co, the resistivity of the spin-up conducting electrons is significantly lower than that of spin-down conducting electrons. When the magnetic moments of the two Co layers are parallel, the conducting electrons that carry the majority of the current in both layers have the same spin orientation. Since the thickness of the GMR stack must be smaller than the electron mean free path, the conducting electrons move through both layers. When the magnetic moments are antiparallel, a spin-up electron in one layer becomes a spin-down electron in the other layer. Every time a spin-up electron in one Co layer crosses the Cu interlayer and enters the other Co layer, it is scattered near the Cu interface. This extra scattering near the Cu interface is the reason for the increase in resistance of the antiparallel state.

$\text{Co}_{90}\text{Fe}_{10}$ has a polarization factor of 0.4. However, the magnetic permeability of a permalloy is significantly higher than that of $\text{Co}_{90}\text{Fe}_{10}$. For these reasons, the free layer is, in practice, made of a NiFe/CoFe composite with CoFe interfacing a Cu interlayer to achieve a high magnetic sensitivity and GMR ratio simultaneously¹⁷.

In a simple spin valve structure, the stray field generated by the pinned layer alters the magnetization orientation of the free layer in the quiescent state, producing asymmetry in the read back response between sensing a head-on (north-pole) and tail-on (south-pole) transition. In today's spin valve read sensors, the pinned layer is replaced by a trilayer structure called a synthetic antiferromagnet (SAF), which consists of two ferromagnetic layers separated by a thin nonmagnetic interlayer (Fig. 6). In a SAF, there is strong interlayer antiferromagnetic exchange coupling, which forces the magnetic moments of the two magnetic layers antiparallel¹⁸. Replacing the pinned layer with a SAF eliminates the stray field on the free layer if the magnetic moments of the two ferromagnetic layers exactly match. A typical example, NiFe/CoFe/Cu/CoFe/Ru/CoFe/PtMn, has CoFe/Ru/CoFe as the SAF. The CoFe layer in the SAF adjacent to the PtMn layer is pinned by the exchange bias field perpendicular to the air-bearing surface, while the other CoFe layer, the reference layer, performs the function of the original pinned layer as a reference to the free layer magnetization orientation (Fig. 8).

Since the total thickness of a NiFe/CoFe/Cu/CoFe spin valve stack is $\sim 100 \text{ \AA}$, which is significantly smaller than the electron mean free path, diffusive scattering of the electrons

at the surfaces results in an increase in resistivity. This spin-independent scattering is detrimental to achieving a high GMR ratio. By capping the free layer with a thin oxide layer, such as TaO, and inserting another thin oxide layer, such as CoFeO_x , in the reference CoFe layer, the GMR ratio of a spin valve can be raised from 12% to 20%^{19,20}. The increase in the GMR ratio has been attributed to the enhancement of the specular, i.e. nondiffusive, scattering at the oxide/metal interfaces. The high GMR ratio allows the read sensor to have a high signal-to-noise ratio, critical at deep submicron track widths. The continued increase in GMR ratio over the years is one of the key factors that has kept the read back signal voltage amplitude at almost the same level while the read track width has steadily decreased. The signal amplitude of today's spin valve head is $\sim 1 \text{ mV}$ zero-to-peak at a read track width of $0.2 \mu\text{m}$ and a sense current density of 10^8 A/cm^2 .

The sensor stack is patterned into a finite width with each side abutted by a permanent magnet (PM) film. The PM layer is magnetized horizontally in the cross-track direction and introduces a magnetic field on the free layer. This ensures that the signal field driven magnetization rotation in the free layer is without hysteresis. In the absence of the PM layer, the free layer magnetization at the vertical side edges orients to form edge domains where the magnetization can be either up or down and is, therefore, bistable. Edge domains in the free layer result in hysteresis in the magnetization rotation while sensing recorded transitions.

Because the vertical edges of the free layer need to be magnetized horizontally to yield a hysteresis-free response, the head sensitivity degrades as the track width, already below 200 nm , is reduced²¹. This is because rotating the magnetization in the center of the free layer, while keeping the magnetization at the edges fixed, results in ferromagnetic exchange energy resisting the free layer magnetization rotation. The dependence of the exchange energy on the track width is inverse-quadratic. For track widths below 100 nm , the head sensitivity degradation will become so severe that an alternative head design will be needed. One of the proposed alternatives is the side-reading free design²². In this design, the permanent magnet layer is eliminated. The sensor stack is extended well beyond the track edges where an extra magnetic layer with a thin metallic interlayer is added onto the free layer to form a moment mismatched SAF. The structure quells the free layer response beyond the track edge without suppressing on-track magnetic sensitivity.

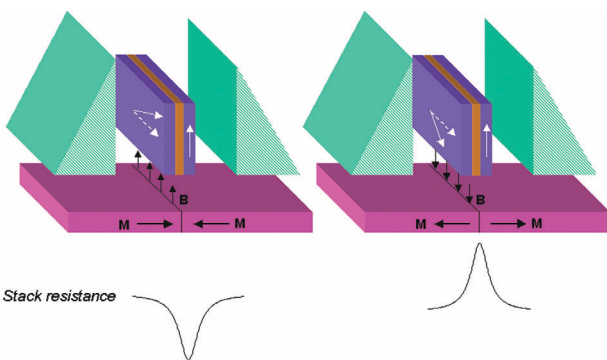


Fig. 8 Schematic of the read back process as a medium with a recorded transition passes over a spin valve read element. The magnetic flux generated by the transition drives the magnetization rotation in the free layer, while the magnetization in the pinned layer is 'fixed' in the perpendicular direction as a reference. Here, a north-pole transition rotates the free layer moment into the moment direction of the reference layer, resulting in a resistance reduction, whereas a south-pole transition results in a resistance increase.

Micromagnetic analysis predicts that the design will enable a well-defined, cross-track profile while maintaining head sensitivity for track widths as narrow as 50 nm. Recent work on fabricating this design has been successful²³.

Beyond spin valves

In spin valve heads, the sense current flows in the film plane across the track width. The signal voltage amplitude is proportional to the track width for a constant sensor stack height. If the sense current can flow perpendicular to the film plane, known as current perpendicular to plane (CPP) mode, reduction of track width will produce no change in the signal voltage amplitude for constant current density. A large GMR ratio in CPP mode was first observed in Co/Ag multilayers²⁴.

The simplest CPP design moves the electric contacts to the top and bottom surfaces of the sensor stack. Because of the large contact area, the resistance of the spin valve stack becomes small. To increase the resistance, a partially magnetic oxide layer is inserted into the Cu interlayer. In addition, nanometer/subnanometer-thick metallic (Cu) layers are inserted in the reference and free layers to raise the GMR ratio by enhancing spin dependent scattering processes²⁵.

Another CPP design consists of a GMR multilayer with magnetostatic coupling and a bias magnet for linearizing the sensor response (Fig. 9)²⁶. Here, the signal field produces a scissoring motion of the magnetic moment in the alternate layers, resulting in a MR signal. The GMR ratio of a CPP multilayer stack can be significantly higher than that of a

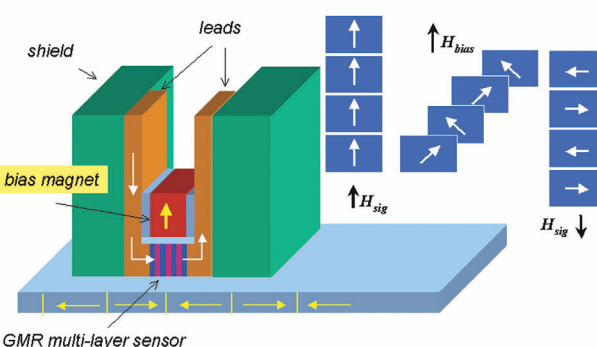


Fig. 9 A CPP/GMR read head design. The sensor is a lithographically patterned GMR magnetic multilayer stack and the sense current flows perpendicular to the film plane of the stack. At the quiescent state, the magnetic moments of adjacent layers scissor at a right angle because of the perpendicular bias field from the biasing magnet and the interlayer magnetostatic coupling. For an upward signal field, the magnetic moments of all the layers will be parallel in the field direction, corresponding to the low resistance state. For a downward signal field, the magnetic moments of adjacent layers will be antiparallel in the horizontal direction, the high resistance state.

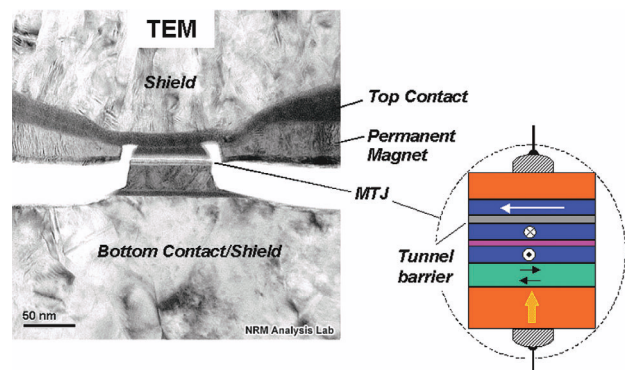


Fig. 10 Cross-section transmission electron micrograph of an MTJ read head and a schematic drawing of its structure. (Transmission electron micrograph courtesy of Sining Mao and Seagate Technology.)

spin valve. This design could be a potential replacement for spin valves in future high area recording density applications.

The magnetic tunnel junction (MTJ) read sensor (Fig. 10) is another promising design for replacing the spin valve²⁷. It has an almost identical structure except that the Cu interlayer is replaced by a thin, 1 nm Al_2O_3 barrier, the electrodes are placed on the top and bottom surfaces of the sensor stack, and the abutted permanent magnets are insulated from the stack to prevent shorting. At a constant bias voltage, the magnitude of the tunneling current through the barrier depends on the relative magnetization orientation of the two adjacent ferromagnetic layers^{28,29}. A tunneling magnetoresistance ratio (TMR), defined in the same way as the GMR ratio, of 41% has been achieved with a $\text{CoFe}/\text{Al}_2\text{O}_3/\text{CoFe}$ structure³⁰. The benefit of a MTJ read sensor is the large signal amplitude because of the relatively high resistance of the tunnel barrier. However, one concern is that shot noise from the tunnel junction may significantly degrade the head signal-to-noise ratio³¹.

Longitudinal thin film recording media

This type of medium, used in current HDDs and made by a sputtering deposition technique, consists of a 1 nm layer of magnetic grains. The grains in most thin film media are CoCrPt alloy, often with an additional element such as Ta^{32,33}. Thin film media, often with additional underlayers, are deposited on Al or glass substrates. Glass is mainly used in mobile applications for withstanding high-g impacts.

The Co-alloy grains in a thin film medium have a hexagonal close packed (hcp) crystalline structure. The magneto-crystalline anisotropy of a grain gives rise to magnetic hysteresis. For each grain, the *c*-axis is the

magnetic easy axis along which the magnetic moment of the grain is in the lowest energy state. Ideally, one would like to have all the grains' *c*-axes aligned along the recording track direction. With a substrate of either Al or glass, the films are polycrystalline and orientation of the grains' easy axes has proven difficult. The random orientation of the grains' *c*-axes is one of the main causes of transition variation in media, known as medium noise. To reduce this randomness, crystalline texture is induced to force all the *c*-axes of the grains to lie within the thin film plane. Depositing the medium onto an underlayer such as Cr orients the in-plane easy axes, as shown in Fig. 11.

Grain boundaries in thin film media are usually Cr-rich, such that they become nonmagnetic. This results in insulation of the ferromagnetic exchange coupling between adjacent grains^{32,34}. In the late 1980s, studies found that intergranular exchange coupling significantly enhances the magnetization variation in recorded transitions^{35,36}. Eliminating intergranular exchange coupling by forming nonmagnetic grain boundaries has been one of the most critical factors in the rapid increase of area recording density³⁷. Substrate heating during film deposition can induce Cr segregation to grain boundaries, while adding elements such as Ta to the alloy can enhance the process³⁸.

Since each grain in thin film media is a magnetic entity, the variation of recorded transitions with location (because of the polycrystalline nature of the film and spatial variation of other magnetic properties) depends on the number of

grains across a data track³⁹. For current thin film media with little intergranular exchange coupling, the transition noise level is inversely proportional to the number of grains across the track. To maintain the signal-to-noise ratio while decreasing track width, grain size (currently ~10 nm in diameter) must be reduced proportionally. Further reduction in grain size, however, encounters an obstacle that could stop the fantastic run of area recording density in recent years.

The energy barrier that preserves the magnetic moment direction in a grain is equal to $K_u V$, the product of the magnetic anisotropy energy constant and the grain volume. If the energy barrier becomes comparable to the thermal energy $k_B T$, where k_B is the Boltzmann constant and T is the absolute temperature, the magnetic moment of the grain can reverse spontaneously under thermal activation, a phenomenon known as superparamagnetism (Fig. 12). This results in the erasure of recorded transitions. To keep data retention time sufficient in a HDD, the following inequality must hold for the energy barrier of a grain⁴⁰,

$$\frac{K_u V}{k_B T} \geq 40$$

For Co-alloy grains, $K_u = 2 \times 10^5$ J/m³, yielding a critical grain diameter of ~9 nm. Further decrease in grain diameter to reduce transition noise demands a proportional rise in the anisotropy energy constant. The dilemma lies in the fact that increasing the anisotropy energy constant will increase the medium coercivity, which is already reaching the limit

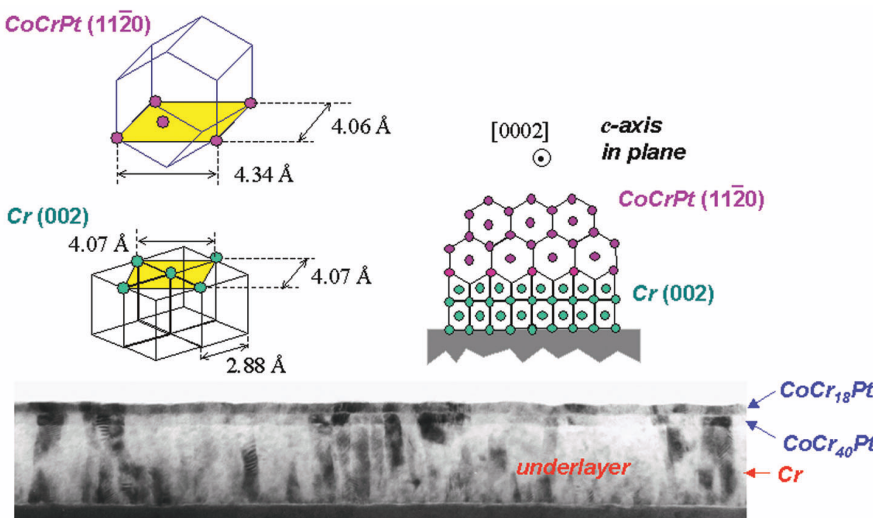


Fig. 11 One of the epitaxial relationships for forcing the *c*-axes of the grains into the film plane. The middle CoCr₄₀Pt is a nonmagnetic layer that has the same crystalline structure as the top CoCr₁₈Pt recording layer. This interlayer helps achieve better epitaxial growth. (Transmission electron micrograph cross-section courtesy of David Laughlin and Yingguo Peng.)

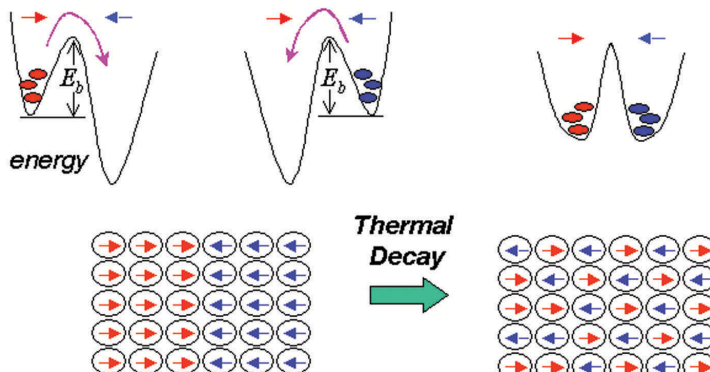
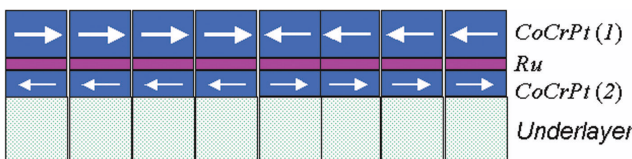


Fig. 12 Spontaneous erasure of a recorded transition under thermal excitation. A transition is in a thermal nonequilibrium state (left) and the asymmetry between the two energy wells is caused by the demagnetization field generated in the transition. Thermal excitation will yield spontaneous magnetization reversal of the grains: when thermal equilibrium is reached, the transition is completely erased. In other words, data retention time in a recording medium is always finite and it is just a matter of how long before data are thermally erased^{35,36}.

imposed by the write head field. For example, the grains in a recently developed, self-assembled FePt medium⁴¹ are 4 nm in diameter with crystalline anisotropy⁴² as high as 6.6×10^6 J/m³. Even though the grains are magnetically stable, the coercivity of the medium could be as high as 5 T, making it impossible to record data using current write heads.

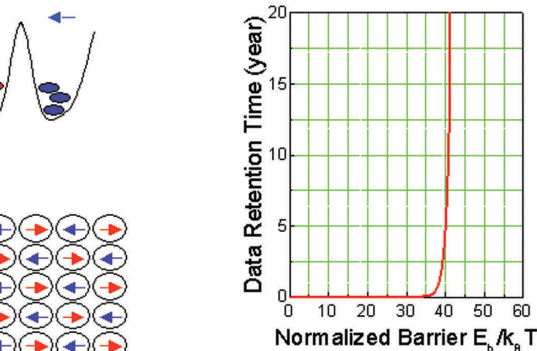
One solution is to keep the volume of each grain unchanged but reduce the grain diameter and increase the medium thickness, i.e. the grain height. However, increasing the medium thickness increases the head-to-medium separation and reduces the head field gradient, consequently broadening the recording transition width. A new type of thin film media – antiferromagnetically coupled media (AFC) – takes an alternative approach by adding a thin layer underneath and a nonmagnetic metal interlayer (Fig. 13)^{43,44}. The grains in the two layers match in the depth direction because of columnar growth during deposition. Interlayer exchange coupling is antiferromagnetic, yielding an antiparallel magnetization configuration in each grain stack.



$$\text{Net moment of a grain: } m = M_{s1}V_1 - M_{s2}V_2$$

$$\text{Net energy barrier: } E_b = K_{u1}V_1 + \alpha K_{u2}V_2$$

Fig. 13 Schematic of an AFC medium. A grain in the lower magnetic layer is weakly coupled to a corresponding grain in the top layer through the Ru interlayer. The Ru layer has the same crystalline structure, hcp, as the CoCrPt layers and the corresponding grains in the two layers have the same crystalline orientation. The effective volumetric increase is a small fraction of the grain volume in the lower layer.



The writing process is determined by the grains in the top layer of relatively weak coupling strength. The coupling effectively adds a small increase to the energy barrier of a top layer grain. Although AFC media are used in current HDDs, extending area recording density beyond what can be offered by single magnetic-layer media is limited.

On the horizon

Are we at the end of what has been a great run for traditional longitudinal recording, or simply at a critical crossroads, ready to adopt a new technology that will lead HDDs to new heights? The latter is likely to be the answer because of the current research efforts under way to develop various novel technologies that may succeed longitudinal recording. The two most attractive ones are perpendicular and heat assisted magnetic recording (HAMR).

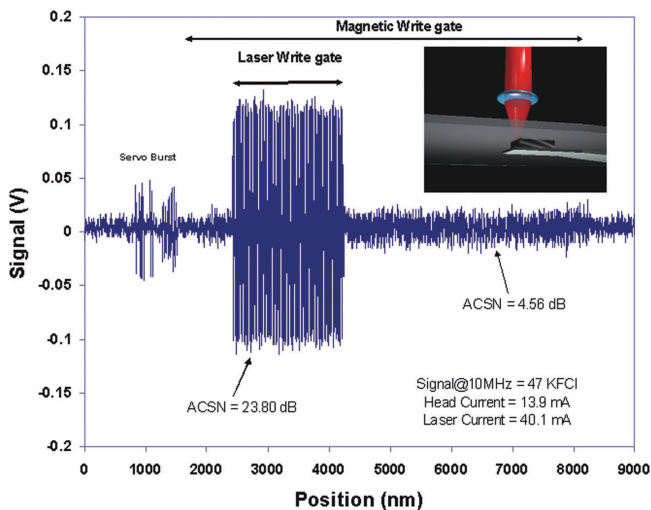


Fig. 15 Proof of concept for HAMR. The inset shows a schematic with a TbFeCo thin film glass disk. A recording head flies over the medium side of the disk and the laser beam illumination from the opposite side heats the medium in the recording zone. The figure shows the read back waveform of the recorded data. When the laser is off, recording with write field alone is not possible. With the laser illumination, data is successfully written into the medium⁴⁸. (Courtesy of Tim Rausch.)

Perpendicular recording was proposed as a replacement more than two decades ago⁴⁵. As shown in Fig. 14, the magnetic moment in the medium is perpendicular to the film plane because of a strong perpendicular magneto-crystalline anisotropy in the Co-alloy grains. The *c*-axes of the grains are aligned perpendicularly with little deviation. In principle, near perfect alignment of the easy axes should yield significantly less noise compared with longitudinal thin film media. The head field, concentrated underneath the write pole-tip, is also in the perpendicular direction. The medium is deposited on a soft magnetic underlayer that provides an efficient return path for the head field flux. The head pole-tip and soft underlayer (SUL) form an effective head gap. Since the medium is within the effective head gap, the write field magnitude should be significantly greater than that in the longitudinal case, provided the pole-tip and SUL separation can be kept smaller than the lateral dimension of the pole-tip footprint. A greater write field enables a larger medium coercivity and, consequently, a higher area recording density, while maintaining sufficient data retention time. Laboratory demonstrations² of perpendicular recording have reached 150 Gbit/in² with the potential for much higher values⁴⁶.

HAMR is an attempt to utilize the strong temperature dependence of magnetic anisotropy^{47,48}. For many types of thin film recording media, increasing temperature can yield a significant reduction in the medium coercivity so that data

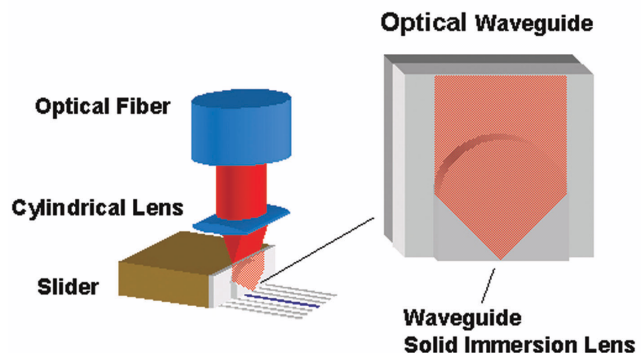


Fig. 16 Schematic of a waveguide solid immersion lens (SIL) integrated onto a slider consisting of a recording head with both write and read elements. The nanometer scale flying height facilitates the near field illumination with an optical spot size defined by the numerical aperture of the SIL. The integration enables the heat spot to coincide exactly with the magnetic writing zone. (Courtesy of Tim Rausch.)

recording can occur at lower write fields. Fig. 15 shows how a thin film medium is used with a laser beam to enable data recording. When the laser light is off, the write field strength is not sufficient to write data into the high coercivity medium. When the laser is on, the coercivity is reduced by the heat generated in the recording zone; the same write head field is then able to write data. In practice, the laser light spot on the medium needs to be the same size as the recording track to avoid disturbance of adjacent tracks. Near-field optics are employed to limit the laser spot size to well below the light wavelength. A waveguide solid immersion lens (SIL) can be integrated into the slider of a recording head (Fig. 16). The spot size in the medium will be essentially defined by the numerical aperture of the SIL.

Conclusion

Over the 46-year history of the magnetic HDD industry, the never-changing goal has been the ability to produce smaller devices with higher storage capacity at a lower cost! Today, HDDs can be purchased for half a cent per megabyte, in contrast with the 1957 cost of about \$10 000. Although HDD technology faces continuing challenges, the unique combination of high storage capacity, low cost, high data transfer rate (presently above 1 Gbit/s), and relatively short seek time (3.5–6 ms) makes it difficult for alternative technologies to take its place. MT

Acknowledgments

The author would like to thank James Bain, Gerardo Bertero, Yingjian Chen, Juren Ding, David Laughlin, Sining Mao, Yingguo Peng, Po K. Wang, and Youfeng Zheng for their contributions to this article. Support from the Data Storage Systems Center and the Department of Electrical and Computer Engineering at Carnegie Mellon University is gratefully appreciated.

REFERENCES

1. Stevens, L. D., In: *Magnetic Recording: The First 100 Years*, Daniel, E. D., et al. (eds.) IEEE Press, New York, (1999), 270
2. Chen, Y., et al., Paper CE-07, Int. Magnetics Conference, Boston, 2003
3. Williams, M. L., and Comstock, R. L., An analytical model of the write process in digital magnetic recording, In: *17th Ann. AIP Conf. Proc.* (1971) 5, 738
4. Bertram, H. N., *Theory of Magnetic Recording*, Cambridge University Press, Cambridge, (1994), 216
5. Bozorth, R. M., *Ferromagnetism*, IEEE Press, New York, (1951), 109
6. Robertson, N., et al., *IEEE Trans. Magn.* (1997) **33**, 2818
7. Bozorth, R. M., *Ferromagnetism*, IEEE Press, New York, (1951), 195
8. Jung, H. S., and Doyle, W. D., *IEEE Trans. Magn.* (2002) **38**, 2015
9. Baibich, M. N., et al., *Phys. Rev. Lett.* (1988) **61**, 2472
10. Dieny, B., et al., *Phys. Rev. B: Condens. Matter* (1991) **43**, 1297
11. Tsang, C., et al., *IEEE Trans. Magn.* (1994) **30**, 3801
12. Yoda, H., et al., *IEEE Trans. Magn.* (1996) **32**, 3363
13. Tsang, C., *IEEE Trans. Magn.* (1989) **25**, 3692
14. Lederman, M., *IEEE Trans. Magn.* (1999) **35**, 794
15. Mott, N. F., *Proc. R. Soc. London, Ser. A* (1936) **153**, 699
16. Soulen, Jr., R. J., et al., *Science* (1998) **282**, 85
17. Kanai, H., et al., *IEEE Trans. Magn.* (1996) **32**, 3368
18. Parking, S. S., *Phys. Rev. Lett.* (1991) **67**, 3598
19. Egelhoff, Jr., W. F., et al., *J. Appl. Phys.* (1997) **82**, 6142
20. Huai, Y., et al., *IEEE Trans. Magn.* (2002) **38**, 20
21. Zhu, J. -G., et al., *IEEE Trans. Magn.* (2001) **37**, 1723
22. Zhu, J. -G., *IEEE Trans. Magn.* (2003) **39**, 576
23. Hasegawa, N., et al., Paper DD-01, Int. Magnetics Conference, Boston, 2003
24. Pratt, W. P., et al., *Phys. Rev. Lett.* (1991) **66**, 3060
25. Saito, M., et al., Paper DD-05, Int. Magnetics Conference, Boston, 2003
26. Rottmayer, R., and Zhu, J., *IEEE Trans. Magn.* (1995) **31**, 2597
27. Mao, S., et al., Paper DC-01, 47th Annual Conference on Magnetism and Magnetic Materials, Tampa, 2002
28. Moodera, J. S., and Kinder, L. R., *J. Appl. Phys.* (1996) **79**, 4724
29. Julliere, M., *Phys. Lett. A* (1975) **54**, 225
30. Cardoso, S., *IEEE Trans. Magn.* (1999) **35**, 2952
31. Araki, S., et al., *IEEE Trans. Magn.* (2002) **38**, 72
32. Johnson, K. E., et al., *J. Appl. Phys.*, (1990) **67**, 4686
33. Utsumi, K., et al., *J. Appl. Phys.* (1997) **73**, 6680
34. Chen, T., and Yamashita, T., *IEEE Trans. Magn.* (1988) **24**, 2700
35. Zhu, J. -G., and Bertram, H. N., *J. Appl. Phys.* (1988) **63**, 3248
36. Zhu, J. -G., *IEEE Trans. Magn.* (1992) **27**, 5040
37. Yoki, T., and Nguyen, T. A., *IEEE Trans. Magn.* (1993) **29**, 307
38. Futamoto, M., et al., *IEEE Trans. Magn.* (1991) **27**, 5280
39. Bertram, H. N., et al., *IEEE Trans. Magn.* (1988) **34**, 1845
40. Charap, S. H., et al., *IEEE Trans. Magn.* (1997) **33**, 978
41. Sun, S., et al., *Science* (2000) **287**, 1989
42. Klemmer, T., et al., *Scripta Metal. Mater.* (1995) **33**, 1793
43. Abarra, E. N., et al., *Appl. Phys. Lett.* (2000) **77**, 2581
44. Fullerton, E. E., et al., *Appl. Phys. Lett.* (2000) **77**, 3806
45. Iwasaki, S., *IEEE Trans. Magn.* (1980) **MAG-16**, 71
46. Bertram, H. N., and Williams, M., *IEEE Trans. Magn.* (2000) **36**, 4
47. Alex, M., et al., *J. Magn. Soc. Jpn.* (2001) **25**, 328
48. Rausch, T., et al., *SPIE Proc. Optical Data Storage Conf.* (2002) **4342**, 502